Atmos. Chem. Phys., 10, 4221–4239, 2010
www.atmos-chem-phys.net/10/4221/2010/
doi:10.5194/acp-10-4221-2010

Atmospheric Chemistry and Physics

Quantifying pollution inflow and outflow over East Asia in spring with regional and global models

M. Lin[1], **T. Holloway**[1], **G. R. Carmichael**[2], **and A. M. Fiore**[3]

[1]Center for Sustainability and the Global Environment (SAGE), Nelson Institute for Environmental Studies, University of Wisconsin, Madison, Wisconsin, USA
[2]Center for Global and Regional Environmental Research, University of Iowa, Iowa City, Iowa, USA
[3]NOAA Geophysical Fluid Dynamics Laboratory, Princeton, New Jersey, USA

Received: 5 December 2009 – Published in Atmos. Chem. Phys. Discuss.: 5 January 2010
Revised: 21 April 2010 – Accepted: 24 April 2010 – Published: 6 May 2010

Abstract. Understanding the exchange processes between the atmospheric boundary layer and the free troposphere is crucial for estimating hemispheric transport of air pollution. Most studies of hemispheric air pollution transport have taken a large-scale perspective using global chemical transport models with fairly coarse spatial and temporal resolutions. In support of United Nations Task Force on Hemispheric Transport of Air Pollution (TF HTAP; www.htap.org), this study employs two high-resolution atmospheric chemistry models (WRF-Chem and CMAQ; 36×36 km) driven with chemical boundary conditions from a global model (MOZART; 1.9×1.9°) to examine the role of fine-scale transport and chemistry processes in controlling pollution export and import over the Asian continent in spring (March 2001). Our analysis indicates the importance of rapid venting through deep convection that develops along the leading edge of frontal system convergence bands, which are not adequately resolved in either of two global models compared with TRACE-P aircraft observations during a frontal event. Both regional model simulations and observations show that frontal outflows of CO, O_3 and PAN can extend to the upper troposphere (6–9 km). Pollution plumes in the global MOZART model are typically diluted and insufficiently lofted to higher altitudes where they can undergo more efficient transport in stronger winds. We use sensitivity simulations that perturb chemical boundary conditions in the CMAQ regional model to estimate that the O_3 production over East Asia (EA) driven by PAN decomposition contributes 20% of the spatial averaged total O_3 response to European (EU) emission perturbations in March, and occasionally contributes approximately 50% of the total O_3 response in subsiding plumes at mountain observatories (at approximately 2 km altitude). The response to decomposing PAN of EU origin is strongly affected by the O_3 formation chemical regimes, which vary with the model chemical mechanism and NO_x/VOC emissions. Our high-resolution models demonstrate a large spatial variability (by up to a factor of 6) in the response of local O_3 to 20% reductions in EU anthropogenic O_3 precursor emissions. The response in the highly populated Asian megacities is 40–50% lower in our high-resolution models than the global model, suggesting that the source-receptor relationships inferred from the global coarse-resolution models likely overestimate health impacts associated with intercontinental O_3 transport. Our results highlight the important roles of rapid convective transport, orographic forcing, urban photochemistry and heterogeneous boundary layer processes in controlling intercontinental transport; these processes may not be well resolved in the large-scale models.

Correspondence to: M. Lin
(mlin26@wisc.edu)

1 Introduction

Pollution export and import from local to global scales is a major concern because of wide-ranging consequences for human health, ecosystems, visibility degradation, changes in radiative forcing, the hydrological cycle, and tropospheric oxidizing capacity. Findings from numerous observational and modeling studies indicate that atmospheric composition throughout the Northern Hemisphere is affected by emissions from upwind continents (e.g. Jaffe et al., 1999, Lelieveld, et al., 2002; Stohl et al., 2002; Fiore et al., 2002; Akimoto, 2003). Wind speeds generally increase with

height, causing pollutants at higher altitudes to be transported rapidly. Chemical species are relatively long-lived in the free troposphere due to weakened chemical loss and the absence of surface deposition. Therefore, hemispheric transport of atmospheric constituents cannot be understood without greater knowledge of exchange processes between the atmospheric boundary layer and the free troposphere. A number of key processes controlling vertical mass transport have been characterized, including the importance of midlatitude frontal passages (e.g. Cooper et al., 2002, 2004), deep convection (Lelieveld and Crutzen, 1994; Lawrence et al., 2003; Hess, 2005), and orographic forcing over complex terrains (Henne et al., 2004; Chen et al., 2009; Ding et al., 2009). The large-scale processes have become better understood in recent years, through integrated analysis of intensive measurement campaigns, satellite data, and ground-based observation networks with models (e.g. Jacob et al., 2003; Heald et al., 2003; Fehsenfeld et al., 2006; Singh et al., 2006., 2009). However, the importance of fine-scale mixing processes, such as by rapid deep convection, dry convection, mountain-valley breezes, and entrainment from the free troposphere into the atmospheric boundary layer, has not been well documented, and these transport mechanisms are often not resolved in global model simulations with a typical resolution of $2^\circ \times 2^\circ$. A number of previous studies suggested that the response of vertical transport and of the distribution of ozone (O_3) and its precursors varies in different models (e.g. Doherty et al., 2005; Lawrence et al., 2003; Kiley et al., 2003; Zhao et al., 2009). Convective systems encompass small-scale fair weather cumuli, active thunderstorms, and meso-scale convective systems (Cotton et al., 1995). The corresponding lifetime of these systems increases with their size from minutes to about half a day. Therefore, the representation of convective transport and associated clouds and precipitation processes need to be parameterized in numerical models and is typically sensitive to both the model's spatial and temporal resolution.

Anthropogenic emissions over Asia have experienced a rapid increase in recent decades (Richter et al., 2005; Zhang et al., 2007). Impacts of Asian emissions on the global environment have been examined through observational and model studies focusing on key export and transpacific processes (e.g. Liu et al., 2003; Carmichael et al., 2003; Cooper et al., 2004), seasonal and episodic variability (e.g. Yienger et al., 2000; Stohl et al., 2002), and impacts over North America (e.g. Fiore et al., 2002; Zhang et al., 2008; Singh et al., 2009; Reidmiller et al., 2009) and Europe (e.g., Stohl et al., 2007; Fiedler et al., 2009). Much less attention has been paid to the import of foreign emissions to Asia. A few studies using global tropospheric chemistry models estimated that European impacts on Asian surface O_3 range from 0.5–5 ppbv for various receptor areas (e.g. Wild et al., 2004; Holloway et al., 2007; Fiore et al., 2009; Jonson et al., 2009). In addition to these model estimates, signatures of European air masses have been detected at a remote mountain site in east Siberia (Pochanart et al., 2003). Compared to pollution export from East Asia and North America, rapid vertical exchange associated with frontal systems is weaker and less frequent over continental Europe (Stohl et al., 2002). The main transport pathway of European pollutants to East Asia occurs predominantly through the boundary layer (Wild et al., 2004), where winds are slower and chemical reactions and surface deposition may lead to additional pollutant loss. Thus, the representation of boundary layer and land surface processes is essential for estimating the import of European pollutants and subsequent impacts on surface air quality over East Asia.

It is not well understood how the key processes in tracer transport, oxidant formation and loss interact at finer temporal and spatial scales. To date, most studies of hemispheric air pollution transport have taken a large-scale perspective: using global chemical transport models (CTMs), focusing on synoptic-scale export events, and evaluating intercontinental source-receptor (S-R) relationships for relatively large regions. Under the United Nations Economic Commission for Europe (UNECE) Convention on Long Range Transboundary Air Pollution (LRTAP), the Task Force on Hemispheric Transport of Air Pollution (TF HTAP; www.htap.org) was established to advance the understanding of hemispheric transport of air pollutants in the Northern Hemisphere. EMEP (European Monitoring and Evaluation Programme) is a scientifically based and policy driven programme under the LRTAP Convention for international co-operation to solve transboundary air pollution problems. Under the umbrella of EMEP and TF HTAP, a set of global and hemispheric CTMs was employed to quantify intercontinental S-R relationships for O_3 (Fiore et al., 2009; Reidmiller et al., 2009; Jonson et al., 2009), oxidized nitrogen deposition (Sanderson et al., 2008), Arctic pollution (Shindell et al., 2008), aerosols, mercury, and persistent organic pollutants (TF HTAP, 2007). Most pertinent to our study are the findings that 8–15% of emitted NO_x is transported over 1000 km from the source region boundaries (Sanderson et al., 2008), sub-continental scale variability in O_3 response to foreign emission changes (Reidmiller et al., 2009) and the wide range in model estimates for EU influence on EA O_3 in spring (over a factor of 2) (Fiore et al., 2009). Continental-scale average estimates of the surface O_3 response to foreign emission changes from the global coarse-resolution models have been used to assess the impacts of intercontinental transport on human health, mortality and crop productivity (Ellingsen et al., 2008; Casper-Anenberg et al., 2009), and will inform global air pollution policy. Thus, it is essential to understand the limitation and uncertainties in estimating S-R relationships using these coarsely resolved models (TF HTAP model resolution ranged from 1 to 5 degree horizontal).

While global CTMs provide an essential framework for estimating intercontinental scale S-R relationships, they often utilize fairly coarse spatial and temporal resolutions and simplified physical and chemical parameterizations because of computational limitations. Higher resolution regional-scale

CTMs generally better simulate regional air pollution meteorology including mixing depth, wind speed, cloud and precipitation patterns, and hence improve the prediction of tracer transport and chemical evolution (e.g., Lin et al., 2008; Lin et al., 2009). In addition, significant uncertainty remains regarding the representation of non-linear urban chemistry relevant to air quality in these global-scale models. Emmerson and Evans (2009) compared an explicit chemical mechanism containing ∼5600 species and ∼13 500 reactions with six simplified tropospheric chemistry schemes utilized in the global models. They found significant uncertainties in the chemical schemes including the treatment of N_2O_5 hydrolysis, PAN formation and sink, isoprene chemistry, and NO_3 nighttime chemistry. Therefore, it is important to evaluate the sensitivity of pollution export, chemical evolution and eventual mixing into surface air over remote regions to model physics and resolution, and to determine how estimated S-R relationships vary within a region (e.g. Lin et al., 2008b; Reidmiller et al., 2009).

We employ two high-resolution regional-scale atmospheric chemistry models – the online-coupled Weather Research and Forecasting model with Chemistry (WRF-Chem v3.0) (Grell et al., 2005) and the Community Multiscale Air Quality model (CMAQ v4.6) (Byun and Schere, 2006) – to examine the export of Asian pollutants to the global atmosphere and the import of European pollution to East Asia. Both models solve for gas-phase and heterogeneous atmospheric chemical processes in a regional, three-dimensional, Eulerian framework, and they represent the two most widely used state-of-the-science models of their kind. To realistically quantify pollution import at the regional boundaries, we apply dynamic boundary conditions of relatively long-lived species derived from the global Model for Ozone and Related Tracers (MOZART v2) (Horowitz et al., 2003). We evaluate MOZART, WRF-Chem, and CMAQ with aircraft observations; examine pollution export processes and the sensitivity of local surface O_3 responses to hemispheric transport. Intercomparison of three different regional and global models in representing pollution import and export permits a greater understanding of how global and regional processes interact, and it allows us to evaluate the role of physical parameterizations vs. resolution in contributing to model uncertainties.

The paper is structured as follows. The models and data used are briefly introduced in Sect. 2.1. We focus our analysis and discussion on three questions: (1) how well did the models represent the observations (Sect. 2.2) (2) how do the regional and global models differ in simulating the surface-to-free troposphere exchange (Sect. 3)? (3) What is the spatial variability of Asian O_3 response to European emission perturbations and the role of direct import of European O_3 vs. production driven by PAN decomposition (Sect. 4)? We then discuss the connection between these regional-to-urban scale processes and hemispheric transport of air pollution, as well as the uncertainty in intercontinental S-R relationships estimated with global models.

2 Model simulations and evaluation

2.1 Meteorological fields and emissions

The WRF regional weather forecasting model is run at 36 km×36 km, with eleven vertical layers in the lowest 2 km and remaining eighteen layers extending to 20 km. The online chemistry component of WRF employs the CBM-Z scheme for gas-phase chemical reactions, the MOSAIC scheme with 4 size bins for aerosol parameterizations, and the Fast-J photolysis scheme coupled with hydrometeors, aerosols and convective parameterizations (Fast et al., 2006 and references therein). The reader is referred to Lin et al. (2009) for a detailed description of the physical options applied in the WRF meteorological predictions. Atmospheric chemical reactions and advection are calculated offline in CMAQ, driven with archived hourly meteorology fields from WRF (hereafter WRF-CMAQ). We choose the SAPRC99/AERO3 scheme for the chemistry of trace gases and aerosols in CMAQ. Regional meteorology should be considered very similar between the two high-resolution air quality models since the feedback of the chemistry to meteorology is not turned on in the WRF-Chem simulations presented here. The key difference between WRF-Chem and WRF-CMAQ lies in the calculation of photolysis rates, gas-phase chemistry, and aerosol dynamics.

The MOZART global model is run at ∼1.9°×1.9° horizontal scale, with 28 levels in the vertical. MOZART is one of the global models participating in the HTAP emission perturbation experiments, which carried out a 20% reduction in anthropogenic emissions from East Asia (EA, 95° E-160° E, 15° N–50° N), Europe (EU, 10°W-50° E, 25° N–65° N), North America (NA, 125°W-60°W, 15° N–55° N), and South Asia (SA, 50° E-95° E, 5° N–35° N) (Fiore et al., 2009). We applied MOZART simulations with base case emissions and with 20% reductions in anthropogenic emissions of O_3 precursors from EU (scenario SR6EU). Each regional model was run twice, with temporally varying (hourly for CMAQ, 6 hourly for WRF-Chem) chemical boundary conditions from the MOZART base and SR6EU simulations, respectively. Boundary conditions consisted of 12 species: O_3, carbon monoxide (CO), peroxyacetyl nitrate (PAN), ethane, propane, acetone, nitrogen oxides (NO_x), sulfur dioxide (SO_2), and speciated aerosols. Ethane, propane, and acetone were selected to represent relatively long-lived non-methane volatile organic compounds (NMVOCs). We evaluate the response in O_3 concentrations over EA due to changes in EU pollutants imported into our regional model domain. This approach builds on previous regional model studies by applying boundary conditions from global models to estimate the impacts of foreign emissions (Carmichael et al., 2007; Lin et al., 2008b). To assess the relative influence of direct transport of EU O_3 vs. local production driven by decomposing PAN of EU origin, we conducted an additional simulation for CMAQ using boundary conditions of PAN and

NO_x from the MOZART base run and other chemical species from the MOZART SR6EU scenario. Differences in EA O_3 concentrations between the above sensitivity simulation and the simulation with all boundary species from the MOZART SR6EU scenario represent the contribution of European PAN to EA O_3 responses. The results are discussed in Sect. 4.

The regional and global models differ in the treatment of boundary layer dynamics and vertical transport processes as well as the spatial and temporal resolutions of driving meteorology. The meteorological fields for 2001 for driving MOZART were taken from the NCEP/NCAR reanalysis and were interpolated from a 6-h time structure to the 20-min time steps of the simulations. The meteorological fields for driving chemistry and transport in the regional models are predicted using the WRF model with 3-min dynamic time steps and with initial and boundary conditions interpolated from the NCEP Final Analysis (FNL, 6 hourly, $1^\circ \times 1^\circ$). Four-dimensional data assimilation was implemented to force the simulated meteorology toward the FNL analysis, and the model was reinitialized every five days to reduce the accumulative errors as discussed in Lin et al. (2009). We choose the Yonsei University (YSU) nonlocal boundary layer vertical diffusion scheme for planetary boundary layer (PBL) parameterizations (Hong et al., 2006) in WRF. The YSU PBL scheme includes an explicit treatment of the entrainment process of heat and momentum at the top of PBL, which resolves two major problems in other PBL schemes: too much mixing with strong wind shear, and too little mixing in the convection-dominated PBL (Hong et al., 2006). Such explicit treatment of the entrainment processes was not implemented in the boundary layer scheme of Holtslag and Boville (1993) employed in the MOZART model. Inadequate treatment of entrainment processes at the PBL top may affect the budget of pollution exchange between the boundary layer and the free troposphere. Convective parameterizations in WRF employ an improved version of the Grell-Devenyi ensemble cumulus scheme (Grell et al., 2002) – Grell-3d, which allows for subsidence in neighboring columns. The MOZART model diagnoses convective mass fluxes using the shallow and midlevel convective transport of Hack (1994) and deep convection scheme of Zhang and McFarlane (1995).

All models employ biomass-burning emissions from the Global Fire Emission Database (GFED v2) (van der Werf et al., 2006). Both CMAQ and WRF-Chem adopt fossil fuel emissions from Streets et al. (2003), updated for the year 2001 as described in Carmichael et al. (2007). Fossil fuel emissions in MOZART are based on EDGAR v2.0 and so representative of the early 1990s (Horowitz et al., 2003). Biomass burning emissions in MOZART are distributed vertically up to 4 km with 70% of these emissions occurring below 2 km, other emissions for all three models are constrained in the surface model layer. Comparing the global and regional model inventories, we find that the large-scale patterns of major O_3 precursors are similar between the two inventories, with the regional inventory estimating higher emissions from urban areas and power plants (Supplementary Fig. S1, http://www.atmos-chem-phys.net/10/4221/2010/acp-10-4221-2010-supplement.pdf). Total emissions of NO_x and CO in the regional emission inventory are ∼15% and ∼5% higher, respectively (Table 1). Total emissions of NMVOCs are close between MOZART and CMAQ, but are ∼50% lower in WRF-Chem. WRF-Chem employs an online biogenic VOC emissions module based on Simpson et al. (1995) and Guenther et al. (1994), and we find that calculated isoprene concentrations over Southeast Asia in WRF-Chem are lower by a factor of 2–5 than CMAQ (Supplementary Fig. S2, http://www.atmos-chem-phys.net/10/4221/2010/acp-10-4221-2010-supplement.pdf), which uses offline biogenic VOC emissions from the POET database for 2000 (Granier et al., 2005; Oliver et al., 2003). Anthropogenic VOC emissions are also approximately 15% lower in WRF-Chem since the CBM-Z chemical scheme considers a smaller set of VOC species than the SAPRC99 mechanism used in CMAQ. Discrepancies in VOC emissions and speciation in the models partly contribute to the bias of O_3 predictions and responses to emission perturbations, and will be discussed in the remaining sections.

Table 1. Total emissions of ozone precursors over East Asia (15–50° N, 95–160° E) in March in the individual models.

MODEL	NO_x (Gg N)	CO (Gg)	NMVOC (Gg C)
MOZART	404.8	12157.5	2445.0
WRF-Chem	453.2	12775.5	(1058.1)[a]
CMAQ	464.8	13307.5	2516.4 (1258.2)[a]

[a] Anthropogenic (including biomass burning) NMVOC emissions are given in parenthesis. Biogenic emissions in WRF-Chem are calculated online, thus are not included here. Supplementary Figs. S1 and S2 (http://www.atmos-chem-phys.net/10/4221/2010/acp-10-4221-2010-supplement.pdf) compare the spatial distributions of anthropogenic and biogenic emissions, respectively.

2.2 Overall model evaluation

Evaluating models with observations is essential for establishing credibility in all applications of model results. Our study focuses on March 2001 since intercontinental transport is generally strongest in the Northern Hemisphere spring season (Yienger et al., 2000; Wild et al., 2004; Stohl et al., 2002). Focusing on March 2001 also gives us an opportunity to evaluate the representation of pollutant export and chemical evolution in regional and global models against intensive measurements obtained from the TRACE-P (Transport and Chemical Evolution over the Pacific) campaign (Jacob et al., 2003). Whereas CMAQ has been well evaluated in prior studies examining chemistry and transport over East Asia (e.g. Uno et al., 2003; Zhang et al., 2004; Lin et al., 2008a,

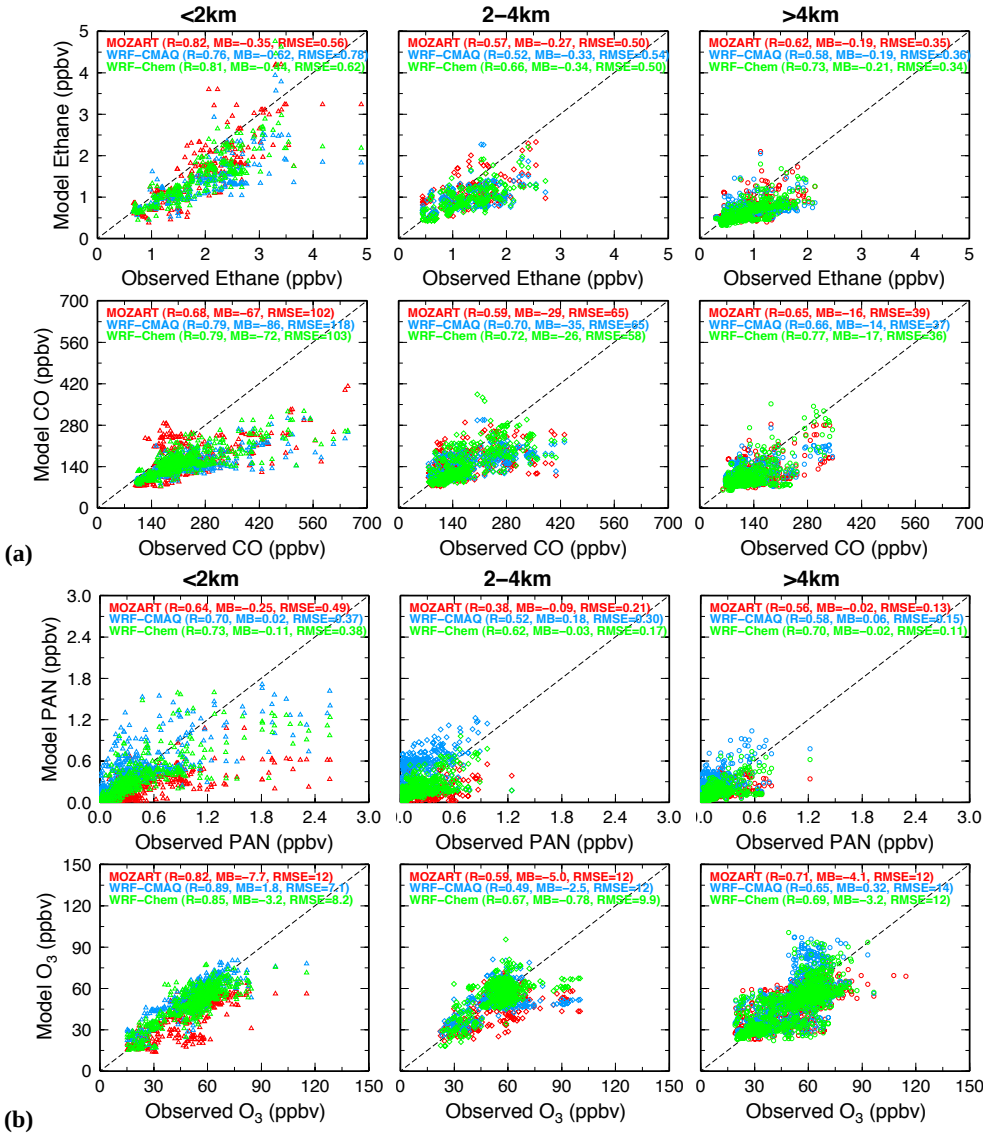

Fig. 1. (a) Comparison of measured (5-min merged) and modeled CO and ethane along the TRACE-P flight tracks in March 2001. Scatter plots are shown for flight sections at altitudes below 2 km (left panel), 2–4 km (middle panel), and above 4 km (right panel). Data points with stratospheric influences diagnosed by $O_3/CO > 1.25$ are omitted. Correlation coefficient (R), mean bias (MB, in ppbv) and root mean square error (RMSE, in ppbv) are calculated for each model: MOZART (red), WRF-CMAQ (blue), and WRF-Chem (green). **(b)** As (a), but for photochemical oxidants O_3 and PAN.

2009), few studies to date have presented WRF-Chem results for this part of the world (Tie et al., 2009; Matsui et al., 2009). Here, we give an overall evaluation of WRF-CMAQ, WRF-Chem, and MOZART against TRACE-P aircraft measurements, and a forthcoming manuscript (hereafter referred to as Lin et al., 2010) will expand the intercomparison and evaluation of WRF-Chem and WRF-CMAQ over East Asia.

The models were sampled every five minutes along the flight tracks. Figure 1 shows the scatter plots of observed and modeled major tracer species (CO and ethane) and photochemical oxidants (O_3 and PAN) at altitudes below 2 km, 2–4 km and above 4 km. Both ethane and CO react relatively slowly in the gas phase and are not efficiently removed by wet processes, thus their distributions reflect mainly the source distribution and transport pathways. All models reproduce well the variations of observed ethane and CO along the flight tracks with correlation coefficients of 0.6–0.8, suggesting that large-scale transport processes were well

captured in the models. Mixing ratios of CO are underestimated by a factor of two below 2 km, consistent with prior studies suggesting that CO emissions from China are higher than assumed in the TRACE-P inventory (Streets et al., 2003; Carmichael et al., 2003; Streets et al., 2006 and references therein). WRF-Chem gives the greatest correlation coefficients with observations of CO and ethane among all three models, indicating the improved ability of the online-coupled climate-chemistry model to resolve more sharply the temporal variation of regional meteorology and associated chemical evolution. Section 3 will further discuss the mechanisms explaining model behavior, in particular the large differences between regional and global models in simulating vertical transport of chemical species.

Larger differences are found in the models' simulation of the main photochemical products, O_3 and PAN (Fig. 1b), than in CO and ethane (Fig. 1a). This divergence in model estimates suggests that important questions remain regarding the complex photochemical processes involving NO_x and VOC precursors. The two regional models give higher regression coefficients than the MOZART global model, as would be expected, given the ability of CMAQ and WRF-Chem to resolve more sharply the spatial gradients in the short-lived O_3 and PAN precursors. We find that MOZART generally underestimates the production of boundary layer O_3 and PAN in springtime, although the HTAP global model intercomparison found that most models, including MOZART, overestimate summertime O_3 (Fiore et al., 2009). Comparing the two regional models, we find that CMAQ gives better statistical scores for O_3 below 2 km, while WRF-Chem better simulates observed O_3 and PAN from 2-4 km. For near surface O_3 below 2 km, CMAQ shows correlation coefficient of R=0.89 and mean bias of MB=1.8 ppbv as compared to R=0.85 and MB=−3.2 ppbv for WRF-Chem. WRF-Chem's underestimate of boundary layer O_3 likely reflects lower VOC emissions from both anthropogenic and biogenic sources included in the simulation (Table 1).

Figure 1b indicates significant variations in the calculated concentration of PAN among the models. The magnitude and variation of PAN mixing ratios along the flight tracks are generally well reproduced in the WRF-Chem model with correlation coefficients of 0.6–0.7 and a negative mean bias $<$0.1 ppbv. MOZART underestimates PAN at all altitude levels. CMAQ predicts the highest concentrations of PAN, and tends to overestimate the observed PAN levels between 2–4 km altitudes. We find that the positive bias of PAN in CMAQ tends to occur in the low-level postfrontal outflow sampled during TRACE-P and often correlates with O_3 underestimates in the same airstreams (figure not shown). The negative correlation between PAN and O_3 suggests that CMAQ's underestimate of O_3 in the postfrontal outflow is likely due to the excessive NO_x uptake by PAN. Lin et al. (2009) reported that CMAQ with the SAPRC99 chemical mechanism predicted 50% higher concentrations of surface PAN over polluted regions than with the Carbon Bond IV (CBIV) mechanism. The SAPRC99 mechanism includes peroxy propionyl nitrate (PPN) and other higher alkyl PAN analogues in addition to PAN, and has explicit treatments of major PAN precursors – acetaldehyde, glyoxal, methylglyoxal, and separate ketone species (ACET, MEK, MVK). Our evaluation with TRACE-P aircraft measurements reveals that SAPRC99 somewhat agrees better than the carbon-bond mechanism in simulating the higher PAN mixing ratios in polluted surface air masses, but overestimates PAN at cleaner conditions above 2km, consistent with the evaluation with INTEX-B aircraft measurements over the eastern Pacific presented by Adhikary et al. (2010). The errors may come from PAN-forming VOC emissions (including biogenic isoprene) and speciation, the thermal decomposition rate, the PAN+OH sink, and other rate constants. The variations in model calculated PAN will affect estimates of the long-range transport of reactive nitrogen and hence O_3 production over remote regions. This will be discussed in Sect. 4.

3 Export of Asian pollutants

Midlatitude cyclones tracking from west to east have been recognized as the primary mechanism for rapidly exporting air pollution from Asia and North America to downwind continents (Cooper et al., 2002, 2004; Stohl et al., 2002). Questions remain, however, as to the amount of surface emissions that make their way to the free troposphere. Here, we examine the importance of both synoptic and fine-scale venting processes in controlling the total budget of Asian emissions exported to the free troposphere as represented in WRF-Chem, WRF-CMAQ and MOZART. Chemistry is dynamically solved online in WRF-Chem without any interpolation of meteorological fields, while both CMAQ and MOZART are driven with temporally interpolated meteorological fields (1-h to 12-min for CMAQ and 6-h to 20-min for MOZART). Therefore, we focus our analysis and discussion of export processes on the comparison of WRF-Chem and MOZART results (Figs. 2, 3, 4, and 6) to highlight the role of model temporal and spatial resolutions. Figure 5 and supplementary Fig. S4 (http://www.atmos-chem-phys.net/10/4221/2010/acp-10-4221-2010-supplement.pdf) present WRF-CMAQ results analogous to those of WRF-Chem, and the difference between the two regional models is also discussed below.

3.1 Episodic nature of Asian outflow

An important feature of the East Asian winter monsoon is frequent southeastward intrusion of cold air triggered by the Siberian anticyclone. Along with the propagation of cold fronts over China and Japan, a midlatitude synoptic wave sweeps northeastward over the East Asian coast. We identified a total of five major frontal events during the March 2001 study period, diagnosed by the decrease in daily mean surface temperature (Liu et al., 2003). Figure 2 compares

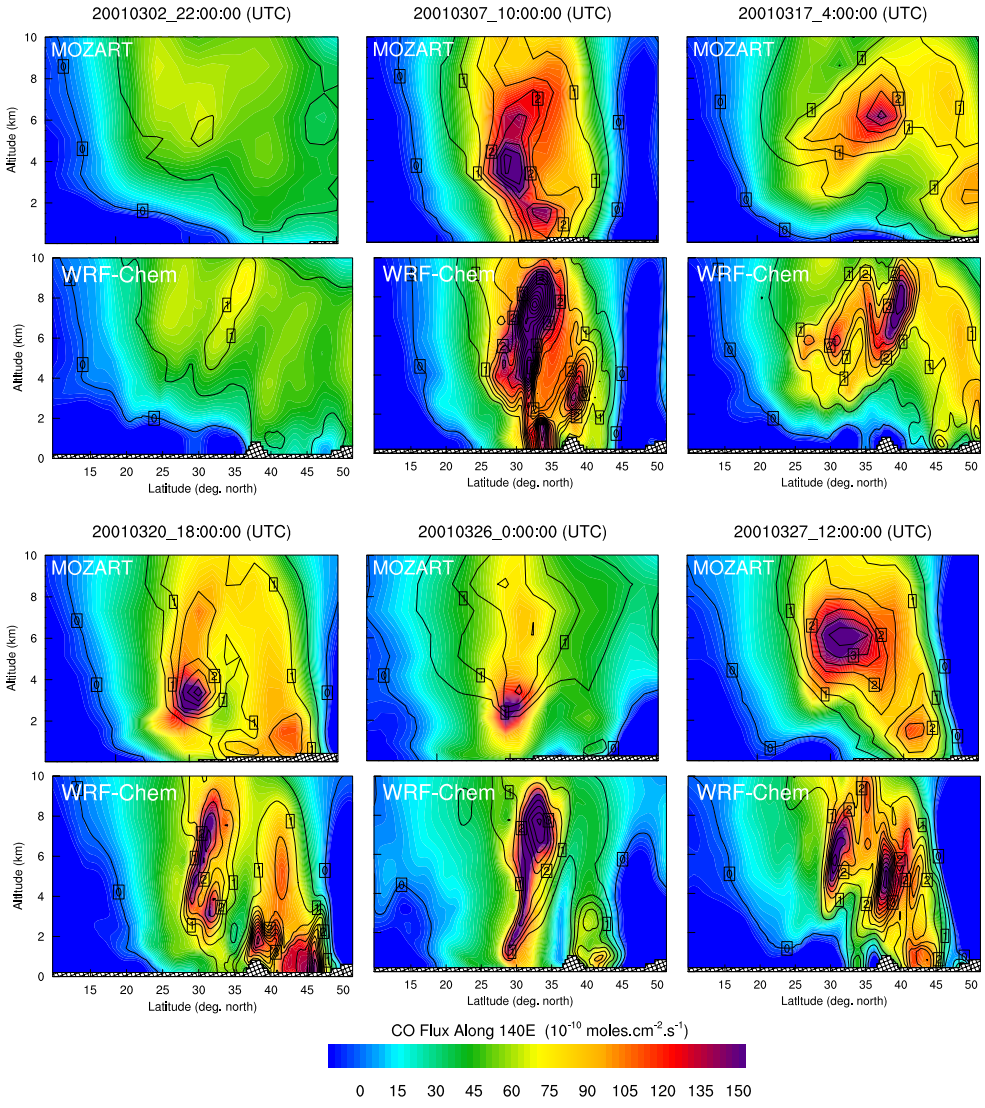

Fig. 2. Comparison of MOZART and WRF-Chem simulated zonal fluxes of CO (filled color) and PAN (contours 0. To 7.5 by 0.5×10^{-11} moles cm^{-2} s^{-1}) along 140° E for selected Asian outflow episodes. Other six episodes are shown in the supplementary Fig. S3 (http://www.atmos-chem-phys.net/10/4221/2010/acp-10-4221-2010-supplement.pdf).

MOZART and WRF-Chem calculated vertical profiles of CO and PAN zonal fluxes along 140° E for six frontal outflow events. The comparison for other six episodes is presented in the supplementary Fig. S3 (http://www.atmos-chem-phys.net/10/4221/2010/acp-10-4221-2010-supplement.pdf). A key feature inferred from Figs. 2 and S3 is that pollution plumes in the high-resolution WRF-Chem model tend to have a multiple – layered structure and are generally more intensified in a certain region and located at higher altitudes where they can undergo more efficient transport in stronger winds. In contrast, pollution plumes in the global MOZART model are typically diluted and insufficiently lofted to higher altitudes. For example, the plumes extend to the upper troposphere (4–9 km) in WRF-Chem as compared to the middle troposphere (2–4 km) in MOZART for the episodes of 7, 20, and 26 March. WRF-Chem also predicts stronger boundary layer outflow confined within the 35–45 N latitude bands during the episodes of 18–20 March. The magnitudes of CO and PAN fluxes for some regions differ by up to a factor of two between the two models. Similar patterns are found for CO, PAN, and ethane (figure not shown), suggesting that the major differences between the models are driven by transport. The stronger outflow of PAN to the western Pacific in WRF-Chem implies that the amount of potential O_3 production over downwind regions (e.g. Western US) driven by decomposing PAN in subsiding transpacific plumes will be larger than in MOZART.

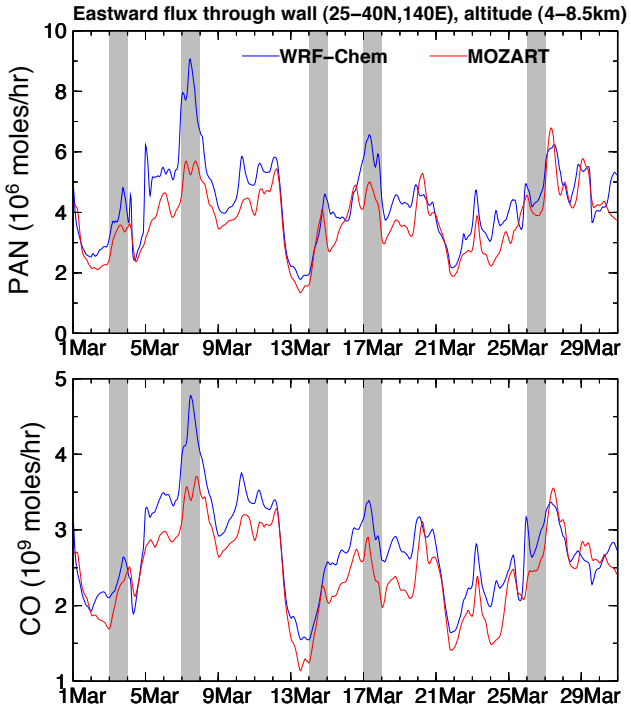

Fig. 3. Comparison of MOZART and WRF-Chem calculated zonal fluxes of CO and PAN along 140° E that is integrated over 4-8.5 km altitudes and 25°–40° N latitudes. The shaded bands indicate the timing of cold frontal passages over central China in March 2001.

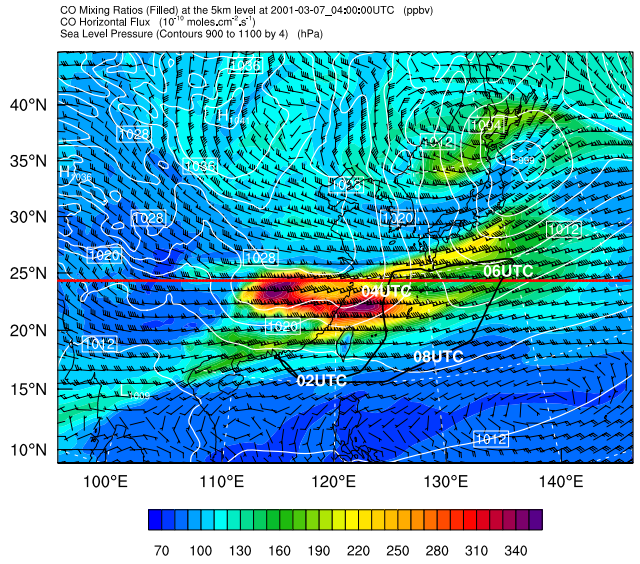

Fig. 4. WRF-Chem simulated CO mixing ratios (filled) and horizontal fluxes (bars) at the 5-km level superimposed with sea level pressure (contours) at 04:00 UTC on 7 March. The red horizontal line approximates the frontal system convergence band, along which a vertical cross-section is shown in Fig. 5. The thick black line labeled with UTC denotes the flight track of the NASA DC8 for which chemical distributions are illustrated in Fig. 6.

Figure 3 illustrates the variation of total fluxes of CO and PAN along 140° E that is integrated from 25–40° N latitudes and from 4–8.5 km altitudes. The 4–8.5 km altitude band is selected to examine the relative pollutant content of air masses transported to the upper troposphere in the models. The shaded bands in Fig. 3 indicate the timing of cold frontal passages over central China, and it should be noted that the shaded area does not necessarily cover the entire outflow episode as the influence of a cold front on pollution outflow may persist over a few days. Outflow of CO and PAN exhibits a strong episodic behavior in association with the passage of midlatitude synoptic waves. Both regional and global models capture elevated frontal outflow, with the WRF-Chem regional model estimating stronger zonal fluxes in the upper troposphere (>4 km). While the global MOZART model can resolve synoptic-scale transport events, the intensity of CO and PAN fluxes is generally weaker than simulated in WRF-Chem. The enhanced lofting of Asian pollutants to higher altitudes as simulated in the WRF-Chem model occurs every 3–4 days throughout the study period.

Total emissions of CO are only 5% higher in WRF-Chem than MOZART, which is not enough to explain the striking discrepancies in the vertical location of pollution plumes as illustrated in Fig. 2. While the injection heights of emissions could contribute to the discrepancy, both anthropogenic and biomass burning emissions are distributed in the surface layer of WRF-Chem so the lofting of pollution to higher altitudes in WRF-Chem is not due to the injection heights of emissions. The greatest discrepancies between the two models are found during 5–8 March when a vigorous cold front swept over East Asia. Calculated total zonal fluxes of CO and PAN are approximately 50% higher in WRF-Chem than in MOZART for this episode. We focus below on this episode, compare model simulated vertical profiles of trace gases with observations, and examine the mechanisms explaining model behavior.

3.2 Role of rapid vertical transport

Figure 4 shows the WRF-Chem forecast of elevated CO in the free troposphere in association with the passage of the cold front on 7 March. A deep cyclone was located over northern Japan (centered at 145° E, 40° N), coexisting with a Siberian anticyclone and a strong convergence band extending from southwest China all the way to northern Japan. We have compared the simulated precipitation pattern in the frontal zone with the multi-satellite data from the Tropical Rainfall Measuring Mission (TRMM) (figure not shown), and their close agreement suggests that the placement, geographical extent, and intensity of this frontal event are well captured by the WRF model. Mixing ratios of CO at the 5-km level reach 200–350 ppbv within the warm conveyor belt, east of the cold front. To identify the origins of the elevated CO in the middle and upper troposphere, we

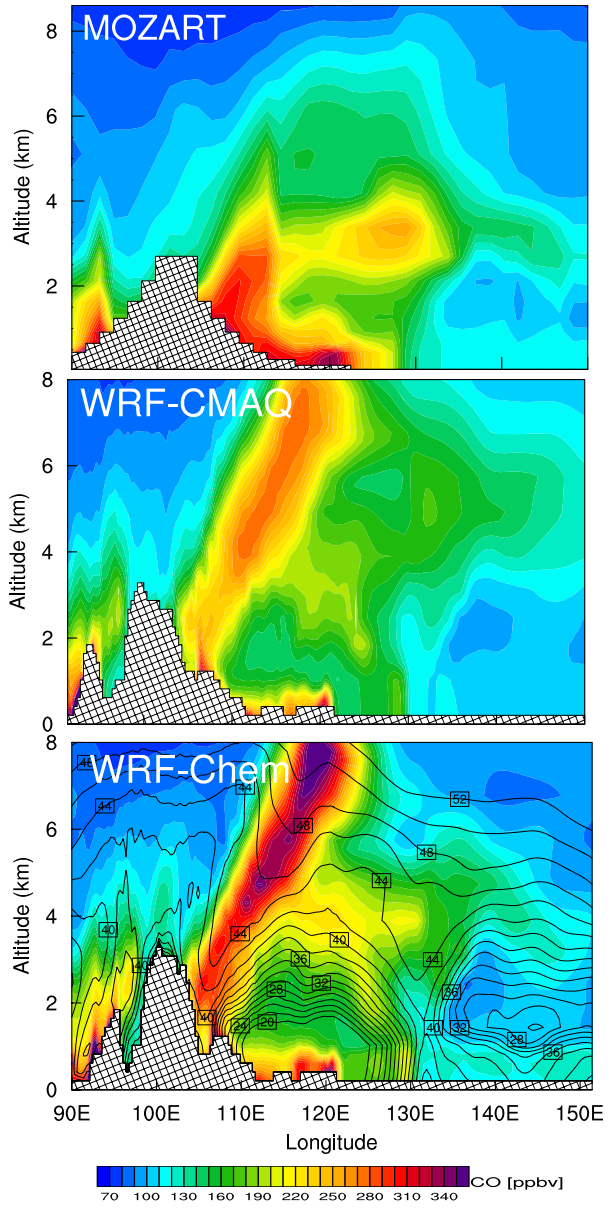

Fig. 5. Comparison of model simulated convective and updraft mixing of CO in association with the passage of the cyclonic wave during 6–7 March. Shown are vertical distributions of CO (filled) and equivalent potential temperature (contours) along the frontal system convergence band indicated in Fig. 4. The hatched areas indicate that surface pressure is below the bottom pressure level used for vertical interpolation.

look at the vertical distribution of CO along ∼25° N, approaching the south side of the convergence zone sweeping over west Myanmar, a heavily burned area in March 2001 (Fig. S1, http://www.atmos-chem-phys.net/10/4221/2010/acp-10-4221-2010-supplement.pdf), and major population centers along the Yangtze River – Chongqing, Wuhan, and Shanghai. Results are shown in Fig. 5 for three models, and we find that the updraft mixing of CO is strongest in WRF-Chem and weakest in MOZART. WRF-Chem predicts strong CO updrafts near Chongqing (105–115° E) extending to the upper troposphere (>4 km) and WRF-CMAQ shows a similar vertical distribution of CO, suggesting that some transport processes were not adequately captured in the global MOZART model, which resulted in a weaker lifting of CO than the two regional models. The WRF-Chem panel in Fig. 5 also shows the vertical distributions of equivalent potential temperature (θ_e), calculated using the formula from Bolton (1980). In stable conditions, θ_e increases with altitude. If θ_e decreases with height, convection can occur, as is the case, above Myanmar (90–100° E) and Chongqing (105–110° E), indicating convective conditions. In particular, deep convection developed near Chongqing, leading to strong upward transport of CO to the upper troposphere in the regional models. The lofting of CO occurred within just a few hours and was rapidly pushed offshore by the strong westerly winds.

This event was sampled by the NASA DC-8 platform flying through the frontal region near the East China coast on 7 March (Fig. 4). Figure 6 compares the observed and modeled vertical distributions of CO, O_3 and PAN along the flight path. It can be seen that the observed CO distributions along the flight path clearly show outflow within the frontal zone (04:00–06:00 UTC) extending to altitudes of ∼6–8 km. Impacts of the primary airstreams that composed this cyclone, e.g. strong advection and lifting in the warm conveyor belt (03:00–06:00 UTC) and dry intrusion of upper level background air (08:00–10:00 UTC), are remarkably well simulated in the high-resolution WRF-Chem model. WRF-Chem predicted outflow of CO to the western Pacific exhibits a complex structure appearing in three vertical layers: mixing of fresh emitted emissions capped in the boundary layer below 1 km; background outflow of CO originated from the coastal region of China confined below ∼3 km over the prefrontal region; and large-scale outflow above 4 km within the frontal zone. While the global MOZART model generally captures the low-level outflow below ∼3 km, the plume in the frontal region (04:00–06:00 UTC) is diluted and appears in the wrong place, strongest in the lower free troposphere (2–4 km) rather than in the middle and upper free troposphere (6–8 km) as in WRF-Chem and in the observations.

The export of CO emissions during the frontal event discussed above is associated with elevated mixing ratios of major photochemical oxidants O_3 and PAN (Fig. 6). Observed mixing ratios of O_3 in the intense CO plume exceed 60 ppbv between 4–8 km (04:00–06:00 UTC), comparable to the low-level outflow confined below 4 km in the prefrontal region, and this observed feature of O_3 enhancement in the frontal region is well captured in the WRF-Chem model. The frontal plume in MOZART (2–4 km, 04:00–06:00 UTC), however, does not show an O_3 enhancement as strong as observed and simulated in WRF-Chem. MOZART somewhat captures the frontal outflow of PAN, but underestimates the observed mixing ratios of PAN by 20–30%.

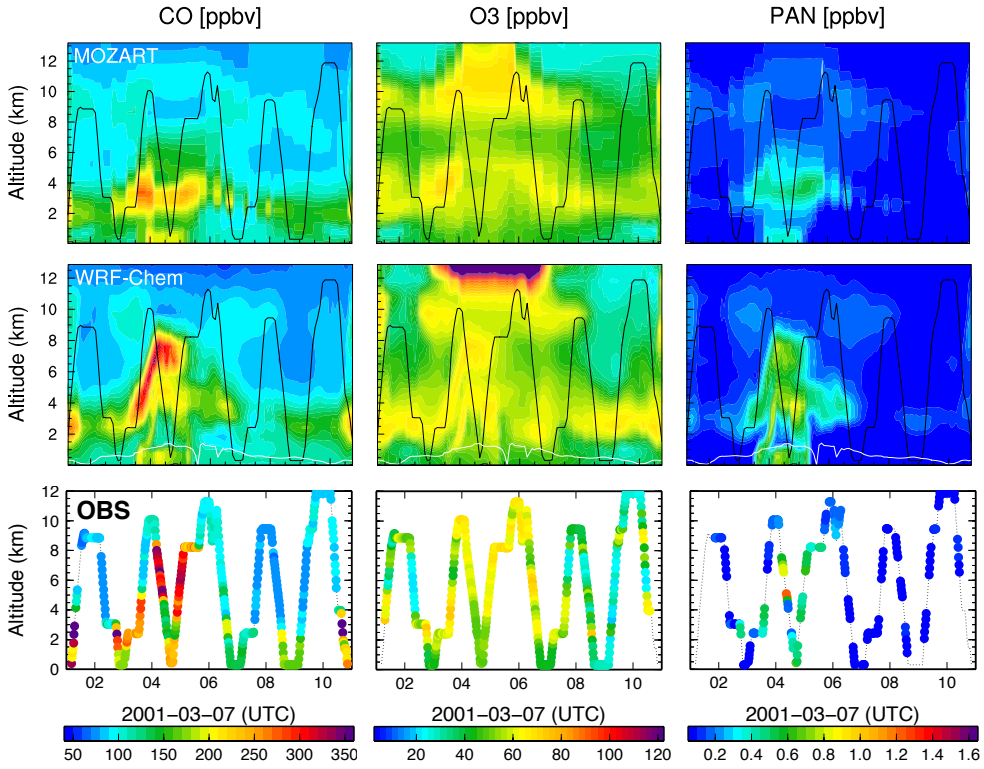

Fig. 6. Observed (1-min merged) and predicted vertical profiles of trace gases along the DC-8 flight track on 7 March during the TRACE-P campaign. The black line denotes the flight path also shown in Fig. 4 with corresponding UTC labels. White lines indicate boundary layer heights.

Figure 5 illustrates a similar vertical transport pattern between WRF-CMAQ and WRF-Chem, and supplementary Figure S4 demonstrates the capability of WRF-CMAQ to capture the timing (04:00-06:00UTC) and location (4-8 km) of DC-8 observed frontal outflow of CO on 7 March. We find that CO mixing ratios in WRF-CMAQ are generally lower by ∼15% than simulated in WRF-Chem. While differences in isoprene emissions could contribute to the discrepancy, the isoprene emissions are larger in WRF-CMAQ (Fig. S2) so the excess CO in WRF-Chem is not due to CO produced during isoprene oxidation. The WRF-Chem model domain covers a larger area of biomass burning region in Southeast Asia (Figs. S1 and S2, http://www.atmos-chem-phys.net/10/4221/2010/acp-10-4221-2010-supplement.pdf). The CMAQ model domain does not include the WRF boundary grid boxes (five in total), and as a result a part of the heavily burned area at the western boundaries has been cut, which partly explains CMAQ's lower estimate of CO mixing ratios in elevated plumes affected by fire emissions. In addition, we suspect that the temporal resolution of convective processes, solved every three minutes in WRF-Chem as compared to the interpolation from a 1-h to 12-min time structure in CMAQ, will play a role in influencing the magnitude of elevated CO.

Sources of CO in the layers above 4 km sampled by the TRACE-P aircrafts are mainly attributable to biomass burning emissions in Southeast Asia (Carmichael et al., 2003) and to industrial emissions along the frontal system convergence bands as illustrated in Fig. 4. All models in this study applied the same dataset for biomass burning emissions (Fig. S1). The striking bias in simulating vertical distributions of trace gases illustrated in Figures 2, 5 and 6 is primarily due to the representation of key meteorological processes in different models. Deep convection is an important mechanism for vertically transporting tropical and subtropical biomass burning emissions out of the atmospheric boundary layer into the middle and upper troposphere (Duncan et al., 2003; Hess, 2005). The occurrence of cold fronts tends to enhance subtropical and tropical deep convection because of the intense low-level convergence along their leading edge (Garreaud, 2001), as is the case simulated in the WRF model. We find consistent enhancement of deep convection embedded in rising airstreams for multiple warm conveyor belt transport events (e.g., 7, 20, 26 March) in March 2001 (figure not shown). MOZART diluted and displaced the plumes at the lower free troposphere for these episodes, suggesting its limited ability to resolve or properly parameterize this rapid deep convection that develops along the leading edge of the frontal system convergence bands. The CO vertical

cross-sections indicate that the updraft mixing of biomass burning emissions from Southeast Asia for some episodes is likely enhanced by orographic forcing over the complex terrains in Myanmar and southwest China (figure not shown). A tracer modeling study by Lin et al. (2010) suggests that the trough (low) formed on the lee side of the Tibetan Plateau and Indochina mountains, is an important transport mechanism for uplifting biomass-burning emissions from Indochina. Other studies have reported that mountain-valley breezes affect the vertical forcing of emissions from polluted Central Eastern China up the nearby mountain slopes (e.g. Ding et al., 2009; Chen et al., 2009).

In summary, meso-scale model studies and supporting observations point out the important roles of deep convection and orographic forcing in enhancing pollution venting during warm conveyor belt lifting events. Inadequate treatment of these transport processes can lead to insufficient lofting of pollution to higher altitudes as seen in the MOZART model. The dilution of intense plumes due to numerical diffusion and coarse resolution in the global-scale models further diminishes the impacts of vigorous episodic transport events (Heald et al., 2003; Wild et al., 2004; Pfister et al., 2006; Fang et al., 2009). Enhanced lifting of surface pollutants to the free troposphere where it can undergo efficient long-range transport – as observed in aircraft studies and simulated in the regional models – might not immediately contribute to the degradation of surface air quality over downwind continents. However, pollutants are generally long-lived in higher altitudes and the mixing into the background troposphere air can eventually lead to increasing levels of background atmospheric constituents over downwind continents (Fiore et al., 2002).

3.3 Uncertainty in export processes

Vertical transport and distribution of tracer species are typically sensitive to the convection schemes used in different models (e.g. Doherty et al., 2005; Lawrence et al., 2003; Kiley et al., 2003; Zhao et al., 2009). The WRF simulations in this study employed the new Grell-3d scheme for convective parameterization (Grell et al., 2002), and evaluation of chemical distributions presented here illustrates the capability of the Grell-3d convection scheme to closely simulate vertical exchanges of air masses. The convective transport schemes of Hack (1994) and Zhang and McFarlane (1995) were applied in both MOZART version 2 (Horowitz et al., 2003) and version 4 (Emmons, et al., 2010). These differences in convective parameterizations likely also contribute to the insufficient lofting of pollution plumes to higher altitudes in the MOZART model.

In addition, high-resolution meteorological fields calculated using the meso-scale models (e.g., MM5, RAMS and WRF), as opposed to the coarse reanalysis data (e.g., NCEP/NCAR, ECMWF) for driving offline global CTMs, further support the improved simulation of tracer vertical transport in the regional scale CTMs. For example, TRACE-P post-campaign analysis showed that the STEM regional model driven with RAMS meteorology ($80\times80\,km^2$, hourly) was also able to capture the elevated CO outflow extending to the upper troposphere for the 7-March episode discussed above (Carmichael et al., 2003), while the global GEOS-Chem model driven with coarse-resolution meteorology ($2^\circ\times2.5^\circ$, 3 hourly) displaced the plume in the lower free troposphere similar to the distribution in MOZART (Liu et al., 2003). Recent model analysis of observations from the 2006 INTEX-B campaign over the Northeast Pacific found that most current global-scale models have limited ability to reproduce discrete Asian gas and aerosol plumes arriving at the North American West Coast (Singh et al., 2009; Dunlea et al., 2009). We suspect that this is partly due to inadequate treatment of small-scale venting over the Asian continent as illustrated in this study and excessive dilution during transpacific transport due to poor resolution in the global-scale models.

We also looked at the vertical profiles of CO at three stations along the East Asian Coast from ten HTAP global models providing vertical profiles for intercomparison and evaluation with ozonesonde observations (Jonson et al., 2010). It appears that none of the global models captured the strong upper-troposphere (6–9 km) CO outflow simulated in WRF-Chem for the 7-March episode, but there is a significant variability of CO vertical profiles among models for the other four frontal episodes in March 2001 (figure not shown). Some events suggest MOZART and WRF-Chem is on the high side of altitudes as compared to the HTAP models and others in the low side, suggesting a real need for more process oriented studies. Among the HTAP global models, MOZECH, CAM-Chem, and CHASER show relatively greater CO outflow to the free troposphere than others. Jonson et al. (2010) examined the vertical profiles of O_3 from the HTAP global models. They found a similar spread in the modeled vertical profiles of O_3 and the agreement between ozonesonde measurements and individual models tends to be at its minimum in spring and summer. The timing and location of pollution plumes may vary among models, but vertical profiles are only available at the individual stations at 12-h intervals and a detailed comparison of HTAP global models is beyond the scope of this study.

Based on available data, we are only able to evaluate model skill at capturing Asian outflow in spring, but we would expect that the fundamental limitations in global model resolution and their ability to resolve subgrid-scale surface-to-free troposphere exchange and chemical processing induce large uncertainties in estimating continental outflow in other regions and seasons. Other studies indicate similar resolution-dependant processes with importance to large-scale continental export. For example, Fang et al. (2009) reported that MOZART underestimated an observed plume with CO in excess of 500 ppbv at 6–10 km from boreal fires during the 2004 INTEX-NA field campaign over

North America by a factor of 5, likely due to excessive dilution of the fire plume or inadequate treatment of pyroconvection that injected strong boreal fire emissions into the upper troposphere and lower stratosphere (Turquety et al., 2007). The smaller-scale venting mechanisms have greatest importance in warm seasons when large-scale stirring by synoptic systems is diminished. Kiley and Fuelberg (2006), using a meso-scale meteorological model (MM5), suggested that weak, midlatitude cyclones in summer are capable of producing vertical lifting as great or greater than much stronger cyclones over North American East Coast. For European outflow, Henne et al. (2004, 2005) revealed a strong influence of topographic venting on O_3 mixing ratios in the lower free troposphere over and downwind of the Alps, and orographic forcing is expected to play an important role in O_3 production and outflow on a European scale.

In addition to transport processes discussed above, there remains a large uncertainty in the outflow of reactive nitrogen (NO_y), including the fraction of individual NO_y species, removal in precipitation associated with frontal lifting and convective processes, and further photochemical processing. The current generation of models captures typical correlations between tracers and NO_y species in the plumes, but the estimate of the NO_y amount transported from the continental boundary layer to free troposphere varies among models (Cooper et al., 2002; Parrish et al., 2004; Li et al., 2004; Sanderson et al., 2008).

4 European impacts over East Asia

We first discuss the spatial sensitivity of monthly mean surface O_3 responses over EA to emission changes in EU (10° W–50° E, 25° N–65° N) (Sect. 4.1). Section 4.2 presents the relative contribution of direct transport of O_3 vs. production driven by PAN decomposition. Section 4.3 discusses time and vertical evolution of EU influences on tropospheric O_3 and CO over China and Japan. We select two regionally representative mountain observatories – Mount Hua (34.5° N, 110.1° E, 2064 m) in central China and Mount Happo (36.7° N, 137.8° E, 1850 m) in central Japan – to demonstrate the temporal evolution of European impacts. Regional air pollution over East Asia and source attributions have been widely examined at Mount Happo in the past decade (e.g., Carmichael et al., 1998; Wild et al., 2004; Lin et al., 2008a, 2009; Tanimoto et al., 2009), and at Mount Hua since the set up of regular O_3measurements in 2004 (e.g., Li et al., 2007; He et al., 2008).

We focus our discussion of European impacts on the model results from CMAQ and MOZART because the two models emit similar quantities of NMVOC, which were found to significantly affect the response of O_3 to emission perturbations (e.g. Fiore et al., 2009). In addition, CMAQ applies hourly-varying chemical boundary conditions, consistent with the output frequency of chemical concentrations in MOZART, while WRF-Chem employs the boundary conditions at six-hour intervals.

4.1 Spatial sensitivity of ozone responses

Figure 7 shows monthly mean O_3 responses over EA to 20% reductions in EU anthropogenic emissions of O_3 precursors. The perturbation in chemical boundary conditions of CMAQ in association with EU emission changes induces a 0.3 ppbv response in spatially averaged surface O_3 over EA. Fiore et al. (2009) reported that the model spread in the EA O_3 response to 20% EU emission reductions is largest in March, ranging from 0.1–0.7 ppbv. The CMAQ estimate falls within the range of global model estimates, but is somewhat lower (0.1 ppbv) than both MOZART and the ensemble mean (0.4 ppbv) of 15 HTAP models.

The large-scale spatial pattern of EU impacts over EA is similar between MOZART and CMAQ. Both models show 0.1–0.2 ppbv stronger response of O_3 in the northwest mountainous regions than the North China Plains (30–45° N, 115–125° E), with the fine-scale model better resolving the sharp orographic gradients. Surface topography can enhance ventilation of surface emissions through mountain-valley wind systems as well as suppress horizontal transport across mountain ridges. Consistent with the results presented here, a few studies reported that the impacts of Asian emissions are strongest on O_3 and PM levels over the Rocky Mountains of the western United States (Jaffe et al., 2003; Reidmiller et al., 2009). Mountain top entrainment of free tropospheric air and weakened surface depositional and chemical loss are key factors contributing to enhanced responses over these regions.

We find a large local and regional variability (by up to a factor of 6) in the EA response to changes in EU O_3 and relevant precursors imported into our regional model domain (Fig. 7b), indicating the important role of surface processes, which differ from region to region. For example, the CMAQ regional model clearly demonstrates the sharp gradients of enhanced O_3 loss through surface deposition over the land, due to uptake by plants and stronger boundary layer turbulence, as opposed to over the ocean. Sharp gradients of coastal lines are not adequately resolved in MOZART, leading to a higher estimate of EU enhancements, as compared to CMAQ, on surface O_3 over the coastal regions of Eastern China, South Korea, and South Japan. Another key feature observed from the regional model results is that EU enhancements appear to be lowest (0.1–0.3 ppbv) over surface air in megacities such as Beijing, Seoul and Tokyo. In these urban areas, European O_3 imported into the regional model domain is titrated by high local emissions of NO_x (Fig. S1, http://www.atmos-chem-phys.net/10/4221/2010/acp-10-4221-2010-supplement.pdf). The global model estimate is 0.4–0.6 ppbv, nearly double than the estimate by the regional model. The large difference over the megacities between the global and regional model results

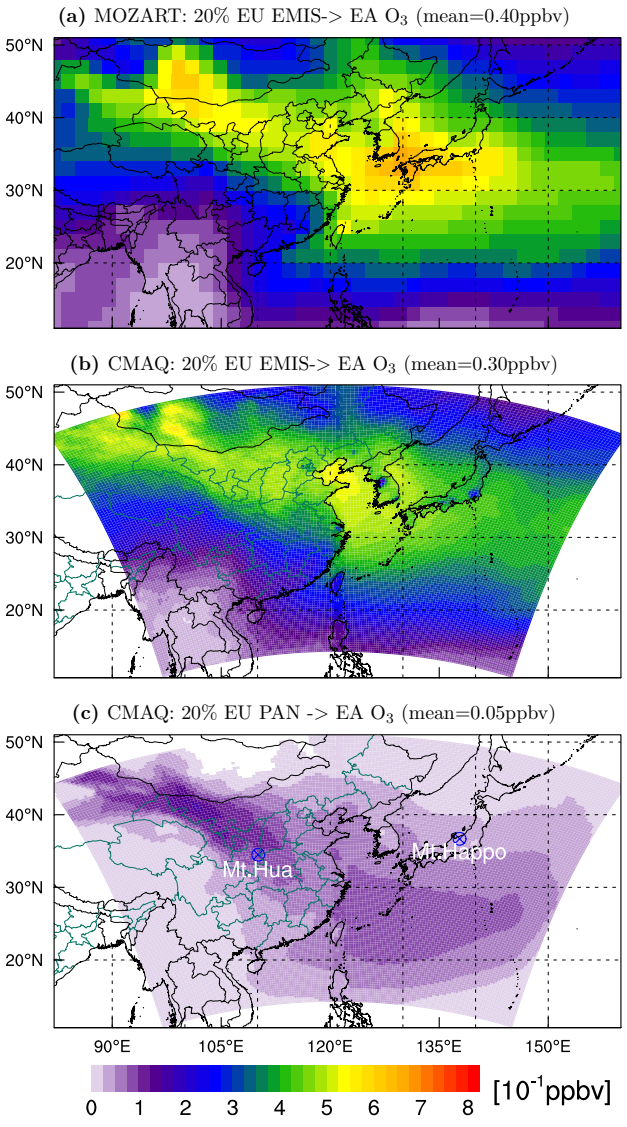

Fig. 7. Monthly mean O_3 response to a 20% reduction in European anthropogenic emissions of O_3 precursors for March 2001. The lower panel shows the contribution of O_3 production driven by PAN decomposition in association with European emission perturbations. Circles denote Mount Hua (34.5° N, 110.1° E) in central China and Mount Happo (36.7° N, 137.8° E) in central Japan

suggests that health impact assessments of foreign emissions using global model results are highly uncertain (e.g., Casper-Anenberg et al., 2009), as 50% of the world's population lives in cities where complex urban photochemistry may fundamentally alter the local impacts of imported pollution, and urban areas are not resolved in the HTAP global models.

4.2 The role of PAN and local chemical regimes

Foreign enhancement on local O_3 budgets can occur either through direct transport of O_3 and/or through production driven by PAN decomposition. PAN acts as an effective reservoir for NO_x, and its thermal decomposition can lead to O_3 production over remote areas far away from emission source regions (Moxim et al., 1996). We conducted sensitivity simulations that perturb PAN boundary conditions in the CMAQ model, and estimate that the contribution of NO_x released from PAN decomposition accounts for nearly 20% of the spatially averaged total O_3 response over East Asia to EU emission reductions (Fig. 7c). To our knowledge, this is the first time that the influence of foreign PAN on local O_3 budgets has been estimated for a region. The contribution of PAN driving O_3 production can reach up to 50% in subsiding plumes in association with cold frontal passages over central China (Mt. Hua – 2064 m) and central Japan (Mt. Happo – 1850 m) (Fig. 8). Consistent with our model results, recent aircraft studies have detected strong O_3 enhancements driven by PAN decomposition in subsiding plumes containing large amount of PAN formed over upwind continents (e.g. Heald et al., 2003; Real et al., 2007; Zhang et al., 2008).

The significant role of PAN in driving O_3 production over remote regions as illustrated in our study indicates that the variation in PAN concentrations simulated in the different models will strongly affect the assessment of intercontinental S-R relationships of O_3. Emmerson and Evans (2009) found that the PAN concentration calculated by six chemical schemes employed in global models varies by up to a factor of five. Our evaluation with TRACE-P aircraft measurements shows that there also exist large uncertainties in regional models' PAN simulations. The MOZART simulation presented in this study underestimates Asian outflow of PAN by 20–30% (Figs. 1b and 6). Fiore et al. (2009) reported a wide range in the NA and EU O_3 response to a 20% decrease in EA emissions, and the response in MOZART is ∼0.1 ppbv lower than the ensemble mean of 15 HTAP models for March. While a variety of factors can contribute to the lower response of O_3 in MOZART, the underestimate of Asian PAN outflow reported here may also play a role.

The chemical regime where the subsiding PAN decomposes determines the O_3 production efficiency and varies with local VOC reactivity and the VOC-to-NO_x ratio. Analysis of aircraft measurements and model sensitivity results suggest that O_3 formation over Northeast Asia is in the NO_x-saturated regime in spring (Carmichael et al., 2003). Thus, increasing NO_x from European sources has a relatively weaker influence on local O_3 production in a model with a lower VOC/NO_x emissions ratio (because of increased termination from OH+NO_2 rather than OH propagation occurring by OH+VOC (Seinfeld and Pandis, 2006)). For example, the WRF-Chem model using the Carbon Bond Mechanism of Zaveri et al. (1999) (CBM-Z) has nearly 15% lower anthropogenic NMVOC emissions and 50% lower from biogenic sources, as compared to either CMAQ or MOZART. This difference likely explains the absence in WRF-Chem of the O_3 enhancements simulated by CMAQ and MOZART during the cold surges of 3–4 and 6–9 March at Mount Hua as well

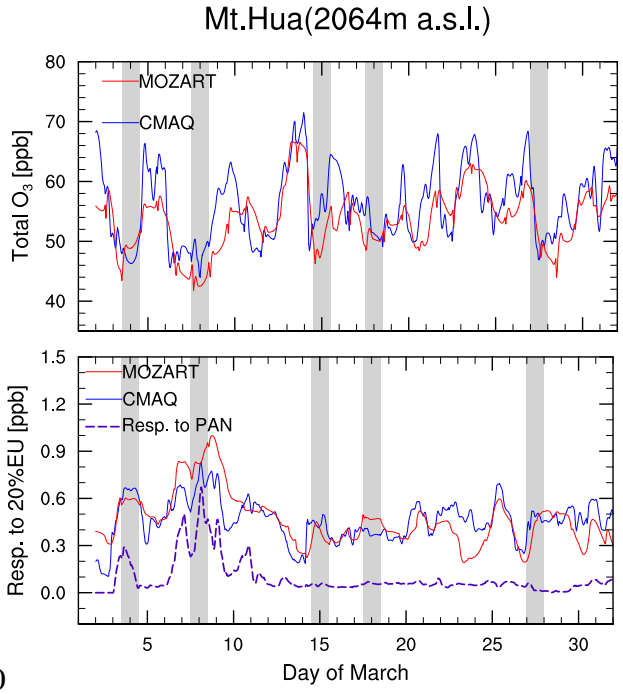

(a)

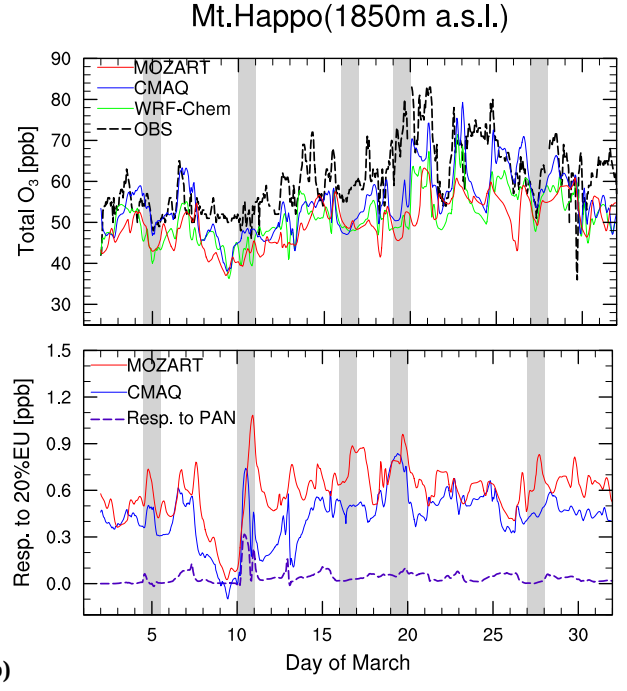

(b)

Fig. 8. **(a)** Day-to-day variability of calculated total O_3 at Mount Hua in central China and Mount Happo in central Japan, and the response to a 20% emission reduction in Europe. WRF-Chem calculated total O_3 and the observations available from the EANET are also shown for Mount Happo. The model results are sampled at the pressure altitude of the mountain sites. The dash purple line represents the contribution of O_3 production driven by PAN decomposition. The shaded bands indicate the timing of cold frontal passages.

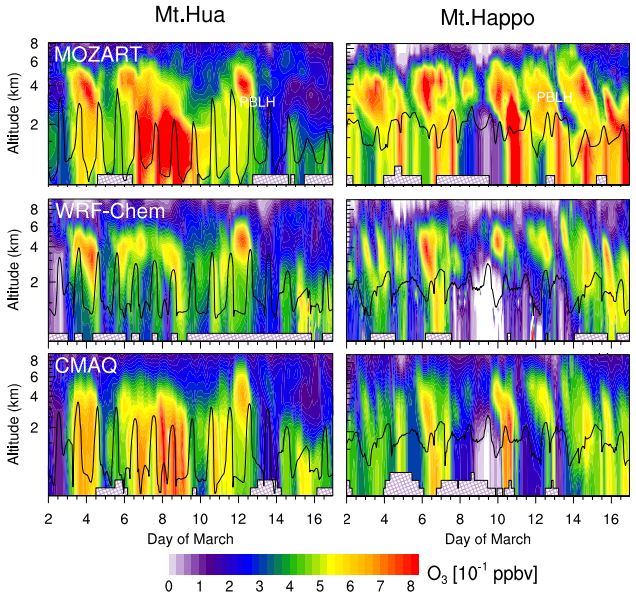

Fig. 9. Time and vertical evolution of O_3 response over China and Japan in association with a 20% perturbation in European emissions. The black line represents boundary layer depths.

as 10–12 March at Mount Happo (Fig. 9). In these subsiding plumes, as much as approximately 50% of O_3enhancements simulated in CMAQ are driven by foreign PAN decomposition (Fig. 8). The CO enhancements are on the same magnitude among the models (Supplementary Figure S6), further supporting that the difference in O_3 enhancements during cold surges is mainly due to the variation in O_3 production efficiency of European NO_x rather than in transport. We conclude that the strength of the local surface O_3 response to reductions in foreign emissions is very sensitive to the chemical regime as represented in the model chemical mechanism.

4.3 Time and vertical evolution of European air masses over East Asia

Figure 8a shows that European influence at Mount Hua is generally strongest (up to 10% of total O_3) on regionally clean days and weakest (<3%) on regionally polluted days, consistent with prior studies for North America (e.g., Fiore et al., 2002). Such a clear negative correlation between European influence and regionally polluted days is not seen at Mount Happo due to the influence of continental outflow from East Asia (in particular the high-O_3 episode on 18–25 March). It should be noted that O_3 measurements at Mount Hua are not available until the year 2004; so observations are only shown at Mount Happo from the Acid Deposition and Monitoring Network in East Asia (EANET) (EANET 2001) (Fig. 8b). All three models reproduced well the observed day-to-day variation of total O_3 at Mount Happo with correlation coefficients

of $R = 0.641$ for WRF-Chem, $R = 0.623$ for WRF-CMAQ, and $R = 0.618$ for MOZART. MOZART underestimated the high-O_3 episode during 18–25 March 2001 by 10–20 ppbv. This O_3 episode was attributed to continental boundary layer outflow from East Asia, and MOZART's underestimate of O_3 at Mount Happo is consistent with its lower CO outflow confined between 35° N–45° N latitudes as compared to WRF-Chem (see 18–20 March snapshots in Figs. 2 and S3, http://www.atmos-chem-phys.net/10/4221/2010/acp-10-4221-2010-supplement.pdf).

The signature of European air masses over Northern China and Japan is demonstrated in CO changes at mountain observatories in response to European emission perturbations (Supplementary Fig. S6, http://www.atmos-chem-phys.net/10/4221/2010/acp-10-4221-2010-supplement.pdf). Regional-scale models (CMAQ and WRF-Chem), by employing chemical boundary conditions from the global model (MOZART), also capture major events of European CO enhancements over China and Japan in association with cold surges. European impacts over Northern China are primarily episodic, and we found five events with 30–50 ppbv enhancements of CO and 3–5 ppbv of O_3 occurring in the atmospheric boundary layer during a single month of March 2001. In contrast, Yienger et al. (2000) estimated that only 3–5 of Asian pollution events directly impacts the atmospheric boundary layer along the US West Coast during a typical February-May period. European air masses exert a greater influence over Japan as compared to Northern China. Due to the influence of southeastward flow over Japan following trans-Eurasia transport in spring (Wild et al., 2004), European emissions also contribute approximately 20–30 ppbv of background CO at central Japan in addition to the episodic impacts of cold surges.

The relationship between boundary layer depths and tropospheric O_3 responses is demonstrated in Fig. 9. A relatively weaker response of O_3 is found in the nocturnal boundary layer for most cases, where O_3 is efficiently removed by surface deposition. During daytime, a mixed layer of vigorous turbulence grows in depth, capped by a statically stable entrainment zone of intermittent turbulence in which small-scale exchanges of chemical species may occur. The three models compared in this study show very different small-scale patterns in the vertical distribution of EU O_3 impacts. While the difference in emissions and chemical regimes discussed previously are most important during cold surges, the representation of entrainment processes in the models may play an important role during other times. Our understanding of intercontinental transport impacts on surface air quality would greatly benefit from further studies of the mixing from the free troposphere into the boundary layer using intensive three-dimensional field measurements and high-resolution models. The California Air Resources Board (CARB), the National Oceanic and Atmospheric Administration (NOAA) and the California Energy Commission (CEC) are proposing a joint field study of atmospheric processes over California and the eastern Pacific coastal region in 2010 (http://www.esrl.noaa.gov/csd/calnex/). Three-dimensional sampling of O_3 and aerosols from lidar, aircraft and research vessel from this study will provide a unique opportunity to examine the entrainment of free tropospheric air into the atmospheric boundary layer and associated influences of orographic flow over the western United States.

5 Conclusions

This study employs two state-of-the-science regional atmospheric chemistry models (WRF-Chem and CMAQ) coupled with a global chemical transport model (MOZART) to examine how chemical transport, oxidant formation and loss interact at finer temporal and spatial scales, and access the sensitivity to model physics. The importance of synoptic to urban scale processes on the rapid export of Asian pollutants and the import of European pollutants over East Asia are evaluated using meteorology for March 2001. While our work was motivated by an interest in the role of regional-scale atmospheric processes and model resolution, it is critical to consider these findings in light of model uncertainties and structure (online vs. offline). Evaluation with intensive aircraft measurements from the TRACE-P field campaign shows that both regional and global models are able to capture the large-scale processes controlling pollution outflow, with the regional models better resolving the fine-scale variability of regional air pollution meteorology and associated chemical processing. There are significant variations in the calculated PAN concentration among models. The ability of the individual model to accurately simulate PAN will affect the long-range transport of reactive nitrogen and hence hemispheric impacts of O_3 pollution. This issue should be further addressed in future studies.

We identified significant differences between regional and global models in simulating vertical mixing of trace gases to the free troposphere and subsequent continental outflow. Our analysis indicates the importance of rapid venting through deep convection that develops along the leading edge of frontal system convergence bands, which are not adequately resolved in either of two global models compared with TRACE-P aircraft observations. Both regional models show that elevated CO, O_3 and PAN extend to the upper troposphere (6–9 km) during a vigorous frontal event. Stronger Asian outflow to the western Pacific and layered structure are simulated in the regional models for multiple events. Given that both WRF-Chem and WRF-CMAQ better match the TRACE-P observations of outflow events, we infer from Figures 2 and S3 that pollution plumes in the global MOZART model are typically diluted and insufficiently lofted to higher altitudes where they can undergo more efficient transport in stronger winds. The difference between regional and global models in simulating tracer vertical transport is much larger than the variation between the online (WRF-Chem)

vs. offline (CMAQ) regional models, suggesting that the limitations in the global models are induced by potential errors in convective parameterizations as well as coarse temporal and spatial resolution. Research needs to be undertaken to further improve the parameterizations of key export processes in large-scale climate-chemistry models, in particular deep convection and the associated cloud and precipitation processes, orographic forcing, and heterogeneous boundary layer processes.

We use sensitivity simulations that perturb chemical boundary conditions in the CMAQ regional model to estimate that the O_3 production over East Asia driven by PAN decomposition contributes 20% of the spatial averaged total O_3 response to European (EU) emission perturbations in March, and occasionally contributes approximately 50% of the total O_3 response in subsiding plumes at mountain observatories (at approximately 2 km altitude). The response to decomposing PAN of EU origin is strongly affected by the O_3 formation chemical regimes, which vary with the model chemical mechanism and NO_x/VOC emissions. Our high-resolution models estimate a 40–50% weaker responses of O_3 in the highly populated Asian megacities to European emission perturbations, as compared to global model estimates. This suggests that the studies using the source-receptor relationships inferred from coarse-resolution global models likely overestimate health impacts associated with intercontinental O_3 transport.

These results imply an important role for dynamic downscaling using regional climate-chemistry models in evaluating global pollution transport, both to advance our understanding of atmospheric processes, and to inform decision-making on air quality management. Future global high-resolution or meso-scale model analysis for a hemispheric domain (e.g. trans-Pacific or trans-Atlantic) should provide further insights into how the export and import processes interact, and help to narrow the uncertainty of intercontinental source-receptor relationships. Major issues that should be addressed in future research include maintaining consistency between regional and global model physics, evaluating the role of physical parameterizations vs. resolution, and developing two-way nesting approaches. In light of the strengths and limitations of each modeling framework, there is a need for further analysis of regional processes affecting global transport and further development of models to improve skill in all key processes. Additional analysis in areas with more extensive measurements of atmospheric constituents at the surface and in the free troposphere would also advance understanding of the hemispheric transport influence on surface air quality.

Acknowledgements. Meiyun Lin and Tracey Holloway were supported on this work by NASA grant NNX07AL36G. TRACE-P data were obtained from NASA Langley Research Center. We are grateful to the Acid Deposition and Oxidants Research Center (ADORC) in Japan for providing EANET data. We thank Claus Moberg and three reviewers for helpful comments in improving the previous version of this manuscript.

Edited by: D. Simpson

References

Adhikary, B., Carmichael, G. R., Kulkarni, S., et al.: A regional scale modeling analysis of aerosol and trace gas distributions over the eastern Pacific during the INTEX-B field campaign, Atmos. Chem. Phys., 10, 2091–2115, 2010, http://www.atmos-chem-phys.net/10/2091/2010/.

Akimoto, H.: Global air quality and pollution, Science, 302, 1716–1719, doi:10.1126/science.1092666, 2003.

Bolton, D.: The computation of equivalent potential temperature, Mon. Weather Rev., 108, 1046–1053, 1980.

Byun, D. W. and Schere, K. L.: Review of the governing equations, computational algorithms, and other components of the Models-3 Community Multiscale Air Quality (CMAQ) modeling system, Appl. Mech. Rev., 59, 51–77, 2006.

Carmichael, G. R., Uno, I., Phadnis, M. J., Zhang, Y., and Sunwoo, Y.: Tropospheric ozone production and transport in the springtime in east Asia, J. Geophys. Res., 103, 10649–10671, doi:10.1029/97JD03740, 1998.

Carmichael, G. R., Tang, Y. and Kurata, G., et al.: Regional-scale chemical transport modeling in support of the analysis of observations obtained during the TRACE-P experiment, J. Geophys. Res., 108(D21), 8823, doi:10.1029/2002JD003117, 2003.

Carmichael, G. R., Sakurai, T., and Streets, D., et al.: MICS-Asia II: the model intercomparison study for Asia phase II: methodology and overview of findings. Atmospheric Environment, 42 (15), 3468–3490, doi:10.1016/j.atmosenv.2007.04.007, 2007.

Casper-Anenberg, S., West, J., Fiore, A., et al.: Intercontinental impacts of ozone pollution on human mortality, Environ. Sci. and Technol., 43(17), 6482–6487, doi:10.1021/es900518z, 2009.

Chen, Y., Zhao, C., Zhang, Q., Deng., Z., Huang, M., and Ma, X.: Aircraft study of mountain chimney effect of Beijing, China, J. Geophys. Res., 114, D08306, doi:10.1029/2008JD010610, 2009.

Cooper, O. R., Moody, J. L., Parrish, D. D., Trainer, M., Ryerson, T. B., Holloway, J. S., Hübler, G., Fehsenfeld, F. C., and Evans, M. J.: Trace gas composition of midlatitude cyclones over the western North Atlantic Ocean: A conceptual model, J. Geophys. Res., 107(D7), 4056, doi:10.1029/2001JD000901, 2002.

Cooper, O. R., Forster, C., Parrish, D., et al.: A case study of transpacific warm conveyor belt transport: Influence of merging airstreams on trace gas import to North America, J. Geophys. Res., 109, D23S08, doi:10.1029/2003JD003624, 2004.

Cotton, W. R., Alexander, G. D., Hertenstein, R., Walko, R. L., McAnelly, R. L., and Nicholls, M.: Cloud venting – A review and some new global annual estimates, Earth-Science Reviews, 39, 169–206, 1995.

Doherty, R. M., D. S. Stevenson, W. J. Collins, and M. G. Sanderson: Influence of convective transport on tropospheric ozone and its precursors in a chemistry-climate model, Atmos. Chem.

Phys., 5, 3205-3218, 2005, http://www.atmos-chem-phys.net/5/3205/2005/.

Ding, A., Wang, T., and Xue, L., et al.: Transport of north China air pollution by midlatitude cyclones: Case study of aircraft measurements in summer 2007, J. Geophys. Res., 114, D08304, doi:10.1029/2008JD011023, 2009.

Duncan, B. N., Bey, I., Chin, M., Mickley, L. J., Fairlie, T. D., Martin, R. V., and Matsueda, H.: Indonesian wildfires of 1997: Impact on tropospheric chemistry, J. Geophys. Res., 108 (D15), 4458, doi:10.1029/2002JD003195, 2003.

Dunlea, E. J., DeCarlo, P. F., and Aiken, A. C., et al.: Evolution of Asian aerosols during transpacific transport in INTEX-B. Atmos. Chem. Phys., 9, 7257–7287, 2009

EANET: Data report on the Acid Deposition in the East Asian Region, 2001, available online at http://www.eanet.cc/product.html, Network center for EANET, 2001.

Ellingsen, K., Gauss, M., Van Dingenen, R., et al.: Global ozone and air quality: a multi-model assessment of risks to human health and crops, Atmos. Chem. Phys. Discuss., 8, 2163–2223, 2008, http://www.atmos-chem-phys-discuss.net/8/2163/2008/.

Emmerson, K. M. and Evans, M. J.: Comparison of tropospheric gas-phase chemistry schemes for use within global models, Atmos. Chem. Phys., 9, 1831–1845, 2009, http://www.atmos-chem-phys.net/9/1831/2009/.

Emmons, L. K., Walters, S., and Hess, P. G., et al.: Description and evaluation of the Model for Ozone and Related Chemical Tracers, version 4 (MOZART-4), Geosci. Model Dev., 3, 43–67, 2010.

Fang, Y., Fiore, A. M., Horowitz, L. W., Gnanadesikan, A., Levy, H., Hu, Y., and Russell, A. G.: Estimating the contribution of strong daily export events to total pollutant export from the United States in summer, J. Geophys. Res., 114, D23302, doi:10.1029/2008JD010946, 2009.

Fast J. D., Gustafson Jr., W. I., Easter, R. C., Zaveri, R. A., Barnard, J. C., Chapman, E. G., and Grell, G. A.: Evolution of ozone, particulates, and aerosol direct forcing in an urban area using a new fully-coupled meteorology, chemistry, and aerosol model. J. Geophys. Res., 111, D21305, doi:10.1029/2005JD006721, 2006.

Fehsenfeld, F. C., Ancellet, G., Bates, T. S., et al.: International Consortium for Atmospheric Research on Transport and Transformation (ICARTT): North America to Europe – Overview of the 2004 summer field study, J. Geophys. Res., 111, D23S01, doi:10.1029/2006JD007829, 2006.

Fiedler, V., Nau, R., Ludmann, S., Arnold, F., Schlager, H., and Stohl, A.: East Asian SO2 pollution plume over Europe – Part 1: Airborne trace gas measurements and source identification by particle dispersion model simulations, Atmos. Chem. Phys., 9, 4717–4728, 2009, http://www.atmos-chem-phys.net/9/4717/2009/.

Fiore, A. M., Jacob, D. J., Bey, I., Yantosca, R. M., Field, B. D., Fusco, A. C., and Wilkinson, J. G.: Background ozone over the United States in summer: Origin, trend, and contribution to pollution episodes, J. Geophys. Res., 107(D15), 4275, doi:10.1029/2001JD000982, 2002.

Fiore, A. M., Dentener, F., and Wild, O., et al.: Mutimodel estimates of intercontinental source-receptor relationships for ozone pollution. J. Geophys. Res., 114, D04301, doi:10.1029/2008JD010816, 2009.

Garreaud, R. D.: Subtropical cold surges: Regional aspects and global distribution, Int. J. Climatol., 21, 1181–1197, 2001.

Granier, C., Guenther, A., Lamarque, J., et al.: POET, a database of surface emissions of ozone precursors, available online at: http://www.aero.jussiue.fr/projet/ACCENT/POET.php, last access: July 2009, 2005.

Grell, G. A., Peckham, S. E., Schmitz, R., McKeen, S. A., Frost, G., Skamarock, W. C., and Eder, B.: Fully coupled online chemistry within the WRF model, Atmos. Environ., 39, 6957–6975, 2005.

Grell, G. A. and Dévényi, D.: A generalized approach to parameterizing convection combining ensemble and data assimilation techniques, Geophys. Res. Lett., 29(14), 1693, doi:10.1029/2002GL015311, 2002.

Guenther, A., Zimmerman, P., and Wildermuth, M.: Natural volatile organic compound emission rate estimates for US woodland landscapes, Atmos. Environ., 28, 1197–1210, 1994.

Hack, J. J.: Parameterization of moist convection in the NCAR community climate model (CCM2), J. Geophys. Res., 99, 5551–5568, 1994.

Heald, C. L., Jacob, D. J., Fiore, A. M., et al: Asian outflow and transpacific transport of carbon monoxide and ozone pollution: An integrated satellite, aircraft, and model perspective, J. Geophys. Res., 108(D24), 4804–4820, doi:10.1029/2003JD003507, 2003

Henne, S., Furger, M., and Nyeki, S., et al.: Quantification of topographic venting of boundary layer air to the free troposphere, Atmos. Chem. Phys., 4, 497–509, 2004, http://www.atmos-chem-phys.net/4/497/2004/.

Henne, S., Dommen, J., Neininger, B., et al.: Influence of mountain venting in the Alps on the ozone chemistry of the lower free troposphere and the European pollution export, J. Geophys. Res., 110, D22307, doi:10.1029/2005JD005936, 2005

He, Y. J., Uno, I., Wang, Z. F., Pochanart, P., Li, J., and Akimoto, H.: Significant impact of the east asia monsoon on ozone seasonal behavior in the boundary layer of eastern china and the west pacific region, Atmos. Chem. Phys., 8(4), 14927–14955, 2008.

Hess, P. G.: A comparison of two paradigms: The relative global roles of moist convective versus nonconvective transport, J. Geophys. Res., 110, D20302, doi:10.1029/2004JD005456, 2005.

Holloway, T., Sakurai T., and Han, Z., et al.: MICS-Asia II: Impacts of global emissions on regional air quality in Asia, Atmos. Environ., 42 (15), 3543–3561, doi:10.1016/j.atmosenv.2007.10.022, 2007.

Holtslag, A. A. M. and Boville, B. A.: Local versus nonlocal boundary layer diffusion in a global climate model, J. Climate, 6, 1825-1842, 1993.

Hong, S. Y., Noh, Y., and Dudhia, J.: A new vertical diffusion package with an explicit treatment of entrainment processes, Mon. Weather Rev., 134, 2318–2341, 2006.

Horowitz, L. W., Walters, S., Mauzerall, D. L., et al.: A global simulation of tropospheric ozone and related tracers: Description and evaluation of MOZART, version 2, J. Geophys. Res., 108(D24), 4784, doi:10.1029/2002JD002853, 2003.

Jacob, D. J., Crawford, J. H., Kelb, M. M., Connors, V. S., Bendura, R. J., Raper, J. L., Sachse, G. W., Gille, J. C., Emmons, L., and Heald, C. L.: Transport and Chemical Evolution over the Pacific (TRACE-P) aircraft mission: Design, execution and first results, J. Geophys. Res., 108(D20), 9000, doi:10.1029/2002JD003276, 2003.

Jaffe, D. A., Anderson, T., Covert, D., Kotchenruther, R., Trost, B., Danielson, J., Simpson, W., Berntsen, T., Karlsdottir, S., Blake, D., Harris, J., Carmichael, G., and Uno, I.: Transport of Asian air pollution to North America, Geophys. Res. Lett., 26, 6, 711–714, 1999.

Jaffe, D. A., Snow, J., and Cooper, O.: The 2001 Asian dust events: Transport and impact on surface aerosol concentrations in the U.S., EOS Transactions American Geophysical Union, 84 (46), 501–516, 2003.

Jonson, J. E., Stohl, A., Fiore, A. M., et al.: A multi-model analysis of vertical ozone profiles, Atmos. Chem. Phys. Discuss., 9, 26095–26142, 2009, http://www.atmos-chem-phys-discuss.net/9/26095/2009/.

Kiley, C. M., Fuelberg, H. E., Palmer, P. I., et al.: An intercomparison and evaluation of aircraft-derived and simulated CO from seven chemical transport models during the TRACE-P experiment, J. Geophys. Res., 108(D21), 8819–8853, 2003.

Kiley, C. M. and Fuelberg, H. E.: An examination of summertime cyclone transport processes during Intercontinental Chemical Transport Experiment (INTEX-A), J. Geophys. Res., 111, D24S06, doi:10.1029/2006JD007115, 2006.

Lawrence, M. G., von Kuhlmann, R., Salzmann, M., et al.: The balance of effects of deep convective mixing on tropospheric ozone, Geophys. Res. Lett., 30(18), 1940–1943, doi:10.1029/2003GL017644, 2003.

Lelieveld, J. and Crutzen, P.-J., Role of deep cloud convection in the ozone budget of the troposphere. Science 264, 1759–1761, 1994

Lelieveld, J., Berresheim, H., Borrmann, S., et al.: Global air pollution crossroads over the Mediterranean, Science, 298(5594), 794–799, doi:10.1126/science.1075457, 2002.

Li, J., Wang, Z., Akimoto, H., Gao, C., Pochanart, P., and Wang, X.: Modeling study of ozone seasonal cycle in lower troposphere over east Asia, J. Geophys. Res., 112, D22S25, doi:10.1029/2006JD008209, 2007.

Li, Q., Jacob, D. J., Munger, J. W., Yantosca, R. M., and Parrish, D. D.: Export of NOy from the North American boundary layer: Reconciling aircraft observations and global model budgets, J. Geophys. Res., 109, D02313, doi:10.1029/2003JD004086, 2004.

Lin, C.-Y., Hsu, H.-M., Lee, Y. H., Kuo, C. H., Sheng, Y.-F., and Chu, D. A.: A new transport mechanism of biomass burning from Indochina as identified by modeling studies, Atmos. Chem. Phys., 9, 7901–7911, 2009, http://www.atmos-chem-phys.net/9/7901/2009/.

Lin, M., Holloway, T., Oki, T., Streets, D. G., and Richter, A.: Multi-scale model analysis of boundary layer ozone over East Asia, Atmos. Chem. Phys., 9, 3277–3301, 2009

Lin, M., Oki, T., Holloway, T., Streets, D. G., Bengtsson, M., and Kanae, S.: Long-range transport of acidifying substances in East Asia – Part I: Model evaluation and sensitivity studies, Atmos. Environ., 42(24), 5939–5955, doi:10.1016/j.atmosenv.2008.04.008, 2008a.

Lin, M., Oki, T., Bengtsson, M., Kanae, S., Holloway, T., and Streets, D. G.: Long-range transport of acidifying substances in Asia – Part II: Source-receptor relationships, Atmos. Environ., 42(24), 5956–5967, doi:10.1016/j.atmosenv.2008.03.039, 2008b.

Liu, H. Y., Jacob, D. J., and Bey, I., et al.: Transport pathways for Asian pollution outflow over the Pacific: Interannual and seasonal variations, J. Geophys. Res., 108(D20), 8786, doi:10.1029/2002JD003102, 2003

Matsui, H., Koike M., Kondo Y., et al.: Spatial and temporal variations of aerosols around Beijing in summer 2006: Model evaluation and source apportionment, J. Geophys. Res., 114, D00G13, doi:10.1029/2008JD010906, 2009

Moxim II, W. J., Levy, H., and Kasibhatla, P. S.: Simulated global tropospheric PAN: Its transport and impact on NO_x. J. Geophys. Res., 101(D7), 12621–12638., 1996.

Olivier, J., Peters, J., and Granier, C., et al.: Present and future emissions of atmospheric compounds, POET report #2, EU project EVK2-1999-00011, available online at, http://www.aero.jussieu.fr/projet/ACCENT/POET.php (last access: July 2009), 2003.

Parrish, D. D., Ryerson, T. B., Holloway, J. S., et al.: Fraction and composition of NO_y transported in air masses lofted from the North American continental boundary layer, J. Geophys. Res., 109, D09302, doi:10.1029/2003JD004226, 2004.

Pfister, G. G., Emmons, L. K., Hess, P., et al.: Ozone production from the 2004 North American boreal fires, J. Geophys. Res., 111, D24S07, doi:10.1029/2006JD007695, 2006.

Pochanart, P., Akimoto, H., Kajii, Y., et al: Regional background ozone and carbon monoxide variations in remote Siberia/East Asia, J. Geophys. Res., 108(D1), 4028–4045, doi:10.1029/2001JD001412, 2003.

Real, E., Law, K. S., Weinzierl, B., et al. : Process influencing ozone levels in Alaskan forest fire plumes during long-range transport over the North Atlantic, J. Geophys. Res., 112, D10S41, doi:10.1029/2006JD007576, 2007

Reidmiller, D. R., Fiore, A. M., and Jaffe, D. A., et al.: The influence of foreign vs. North American emissions on surface ozone in the US, Atmos. Chem. Phys., 9, 5027–5042, 2009, http://www.atmos-chem-phys.net/9/5027/2009/.

Richter, A., Burrows, J. P., Nuss, H., Granier, C., and Niemeier, U.: Increase in tropospheric nitrogen dioxide over China observed from space, Nature, 437(7055), 129–132, 2005.

Sanderson, M., Dentener, F. J., Fiore, A. M., et al.: A multi-model study of the hemispheric transport and deposition of oxidised nitrogen, Geophys. Res. Lett., 35, L17815, doi:10.1029/2008GL035389, 2008.

Seinfeld, J. H. and Pandis, S. N.: Atmos. Chem. Phys.: From Air Pollution to Climate Change, Wiley, New York, USA, 215–225, 2006.

Shindell, D. T., Chin, M., Dentener, F., et al.: A multi-model assessment of pollution transport to the Arctic, Atmos. Chem. Phys., 8, 5353–5372, 2008, http://www.atmos-chem-phys.net/8/5353/2008/.

Simpson, D., Guenther, A., Hewitt, C. N., and Steinbrecher, R.: Biogenic emissions in Europe. 1. Estimates and uncertainties, J. Geophys. Res., 100D, 22875–22890, 1995.

Singh, H. B., Brune, W. H., Crawford, J. H., Jacob, D. J., and Russell, P. B.: Overview of the summer 2004 Intercontinental Chemical Transport Experiment-North America (INTEX-A), J. Geophys. Res., 111, D24S01, doi:10.1029/2006JD007905, 2006.

Singh, H. B., Brune, W. H., Crawford, J. H., Flocke, F., and Jacob, D. J.: Chemistry and transport of pollution over the Gulf of Mexico and the Pacific: spring 2006 INTEX-B campaign overview and first results, Atmos. Chem. Phys., 9, 2301–2318, 2009, http://www.atmos-chem-phys.net/9/2301/2009/.

Streets, D. G., Bond, T. C., Carmichael, G. R., Fernandes, S. D., Fu, Q., He, D., Klimont, Z., Nelson, S. M., Tsai, N. Y., Wang,

M. Q., Woo, J. H., and Yarber, K. F.: An inventory of gaseous and primary aerosol emissions in Asia in the year 2000. J. Geophys. Res., 108(D21), 8809, doi:10.1029/2002JD003093, 2003.

Streets, D. G., Zhang, Q., Wang, L., He, K., Hao, J., Wu, Y., Tang, Y., and Carmichael, G. R.: Revisiting China's CO emissions after the Transport and Chemical Evolution over the Pacific (TRACE-P) mission: Synthesis of inventories, atmospheric modeling, and observations, J. Geophys. Res., 111, D14306, doi:10.1029/2006JD007118, 2006.

Stohl, A., Eckhardt, S., Forster, C., James, P., and Spichtinger, N.: On the pathways and timescales of intercontinental air pollution transport, J. Geophys. Res., 107(D23), 4684, doi:10.1029/2001JD001396, 2002

Stohl, A., Forster, C., Huntrieser, H., Mannstein, H., McMillan, W. W., Petzold, A., Schlager, H., and Weinzierl, B.: Aircraft measurements over Europe of an air pollution plume from Southeast Asia aerosol and chemical characterization, Atmos. Chem. Phys., 7, 913–937, 2007,
http://www.atmos-chem-phys.net/7/913/2007/.

Tanimoto, H.: Increase in springtime tropospheric ozone at a mountainous site in Japan for the period 1998–2006, Atmos. Environ., 43, 1358–1363, 2009.

Tie, X., Geng, F. H., Peng, L., Gao, W., and Zhao, C. S.: Measurement and modeling of O_3 variability in Shanghai, China; Application of the WRF-Chem model, Atmos. Environ., 43, 4289–4302, 2009.

Task Force on Hemispheric Transport of Air Pollution: Hemispheric transport of air pollution 2007 interim report, edited by: Keating, T. J. and Zuber, A., Air Pollut. Stud. 16, UN Econ. Comm. for Europe, New York, USA, 2007.

Turquety, S., Logan, J. A., Jacob, D. J., Hudman, R. C., Leung, F. Y., Heald, C. L., Yantosca, R. M., Wu, S., Emmons, L. K., Edwards, D. P., and Sachse, G. W.: Inventory of boreal fire emissions for North America in 2004: Importance of peat burning and pyroconvective injection, J. Geophys. Res., 112, D12S03, doi:10.1029/2006JD007281, 2007.

Uno, I., Carmichael, G. R., Streets, D. G., et al.: Regional chemical weather forecasting system CFORS: Model descriptions and analysis of surface observations at Japanese island stations during the ACE-Asia experiment, J. Geophys. Res., 108(D23), 8668, doi:10.1029/2002JD002845, 2003.

van der Werf, G. R., Randerson, J. T., Giglio, L., Collatz, G. J., Kasibhatla, P. S., and Arellano, A. F.: Interannual variability in global biomass burning emissions from 1997 to 2004, Atmos. Chem. Phys., 6, 3423–3441, 2006,
http://www.atmos-chem-phys.net/6/3423/2006/.

Wild, O., Pochanart, P., and Akimoto, H.: Trans-Eurasian transport of ozone and its precursors, J. Geophys. Res., 109: D11302, doi:10.1029/2003JD004501, 2004

Yienger, J., Galanter, M., Holloway, T., Phandis, M., Guttikunda, S., Carmichael, G., Moxim, W., and Levy II, H.: The episodic nature of air pollution transport from Asia to North America, J. Geophys. Res., 105(D22), 26931–26945, 2000.

Zaveri, R. A. and Peters, L. K.: A new lumped structure photochemical mechanism for large-scale applications, J. Geophys. Res., 104(D23), 30387–30415, 1999.

Zhang, G. J. and McFarlane, N. A.: Sensitivity of climate simulations to the parameterization of cumulus convection in the Canadian climate centre general circulation model, Atmos. Ocean, 33, 407–446, 1995.

Zhang, L., Jacob, D. J., Boersma, K. F., et al.: Transpacific transport of ozone pollution and the effect of recent Asian emission increases on air quality in North America: an integrated analysis using satellite, aircraft, ozonesonde, and surface observations, Atmos. Chem. Phys., 8, 6117–6136, 2008,
http://www.atmos-chem-phys.net/8/6117/2008/.

Zhang, M. G., Uno, I., Carmichael, G. R., et al.: Large-scale structure of trace gas and aerosol distributions over the western Pacific Ocean during the Transport and Chemical Evolution Over the Pacific (TRACE-P) experiment, J. Geophys. Res., 108(D21), doi:10.1029/2002JD002946, 2003.

Zhang, Q., Streets, D. G., He., K., et al.: NO_x emission trends for China, 1995–2004: The view from the ground and the view from space, J. Geophys. Res., 112, D22306, doi:10.1029/2007JD008684, 2007

Zhao, C., Wang, Y., Choi, Y., and Zeng, T.: Summertime impact of convective t ransport and lightning NO_x production over North America: modeling dependence on meteorological simulations, Atmos. Chem. Phys., 9, 4315–4327, 2009,
http://www.atmos-chem-phys.net/9/4315/2009/.